TIME-RESOLVED EJECTA VELOCITY DISTRIBUTION IN OBLIQUE IMPACTS B. Hermalyn[1], P. H. Schultz[1], J.L.B. Anderson[2] and J.T. Heineck[3], [1]Brown University, Providence, RI 02912-1846 (Brendan_Hermalyn@brown.edu); [2]Winona State University, Winona, MN 55987; [3]NASA Ames Research Center, Moffet Field, CA 94035

Introduction: Prior studies explored the distribution of ejected material for vertical impact events through dimensional analysis [1], numerical simulations [2], and experimental investigations [3,4,5]. Statistically, however, most impacts do not occur at vertical incidence [6]. While many planetary impacts over a range of impact angles result in symmetric final crater shapes, the velocity and mass distributions of the ejecta are not axisymmetric in non-vertical impacts [5,7]. In this study, we present the application of a new technique for determining the time resolved ejecta mass-velocity distribution in oblique impacts.

Data Collection and Technique: Impact experiments were performed at the NASA Ames Vertical Gun Range (AVGR). A new high-speed Three-Dimensional Particle Imaging Velocimetry (3D-PIV) system recorded the ejecta evolution. A laser light sheet parallel to the impact surface illuminated "slices" of the ejecta curtain. The raw images (Fig. 1) from the 3D-PIV system were then processed for: a) cross correlation to identify individual particle motion in the curtain, yielding the velocity of the ejecta [5], and b) particle and area counting of the curtain to calculate ejected mass. Our new system, however, records at a much higher framing rate than prior studies (1000 frames/sec vs. 1 frame/experiment), thus allowing for the non-invasive, time-resolved measurement of the velocity and mass in the expanding ejecta curtain.

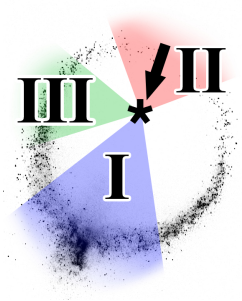

Figure 1: Raw inverted data image from 3D-PIV system. Arrow indicates direction of impact; asterisk denotes impact point. Downrange (I), uprange (II), and lateral (III) ROIs are shaded as in [7].

Analysis and Results: In this study, we divide the expanding ejecta curtain into three regions of interest (ROI): downrange (I), uprange (II), and lateral (III) following [7] (Fig. 1). The data set presented is from a 1 km/s impact of an Al projectile into #20-40 sand at 30° under vacuum conditions. The high-speed 3D-PIV system allows for time-resolved calculation of ejecta velocities throughout the cratering process, from a few milliseconds after impact to beyond the end of crater growth (Fig. 2). This technique also allows the exploration of the ejecta mass through time. The incremental and cumulative ejecta-mass distribution is derived from individual ejecta particles illuminated in the laser sheet. The incremental mass ejected uprange is reduced by three orders of magnitude at T_c and exhibits an ejecta-mass distribution unlike the downrange or lateral regions.

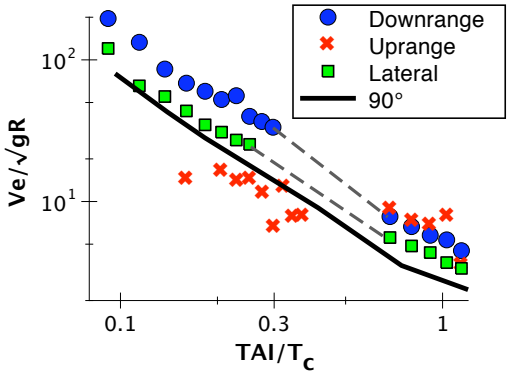

Figure 2: Scaled ejecta velocity as a function of scaled time after impact for ROIs. Data from vertical impact under identical conditions plotted in black. Note that for early stages of crater formation, there is virtually no ejecta in the uprange direction (Zone of Avoidance). All three oblique components have similar trend at end of crater growth. Undersampled region around TAI/Tc~0.5 will be studied using refined timing calibration of 3D-PIV system.

Applications: The new high-speed 3D-PIV system holds promise for reconstructing the ejecta-mass evolution for the *Deep Impact* collision into Comet 9P/Tempel 1 for both and high porosity nominal particulate targets. Additionally, this non-evasive technique permits examining source depths (and possible topographic effects) on ejecta evolution including the effect on crater rays and the uprange heart-shaped ray system [8]. These results will be combined with spectral observations [9] in order to understand the surface structure of Tempel 1.

References: [1] Housen, K.R., et al. (1983) *JGR, 88,* 2485-2499; [2] Wada K. et al. (2006) *Icarus, 180,* 528—545; [3] Morrison, R. H. and Oberbeck, V. R. (1976) *LPI Contributions, 259,* 79; [4] Schultz, P.H. (1996) *LPS XXX,* Abstract #1919; [5] Anderson, J.L.B., et al. (2003) *JGR, 108(E8),* 5094; [6] Gault, D. E. and Wedekind, J. A. (1978), Proc. LPSC IX, 3843-3875.2; [7] Anderson, J.L.B, and Schultz, P.H. (2006) *LPS XXXVII*, Abstract #1726 [8] Schultz, P.H., et al. (2007) *Icarus, 190,* 295-333.; [9] Sunshine, J.M., et al. (2007) *Icarus, 190,* 284-294.